# Supplementary Information

## Three-Dimensional Metal-Free Perovskite with Switchable Dielectric Behaviors

Feng-Wen Zhang,[a] Yu-Lan Xie,[a] Pei-Guo Liu,[a] Meng-Qiang Li,[a] Yi-Xuan Yang,[a] Hao-Fei Ni,[a] Gele Teri,[a] Ming Zhu,[a] Chang-Feng Wang,*[a] Yi Zhang,*[a] and Da-Wei Fu,*[ab]

[a] Institute for Science and Applications of Molecular Ferroelectrics, Key Laboratory of the Ministry of Education for Advanced Catalysis Materials, Zhejiang Normal University, Jinhua 321004, People's Republic of China.

Email: wang1215@zjnu.edu.cn; yizhang1980@seu.edu.cn; dawei@zjnu.edu.cn

[b] Ordered Matter Science Research Center, Jiangsu Key Laboratory for Science and applications of Molecular Ferroelectrics, Southeast University, Nanjing 211189, People's Republic of China.

Email: dawei@seu.edu.cn

## Experimental section

### Materials

All reagents and solvents used in this work were purchased from commercial sources and used without any further purification or modification. Methylpiperazine ($C_5H_{12}N_2$, 98%, Meryer), Ammonium tetrafluoroborate ($NH_4BF_4$, 97%, Macklin) and Fluoboric Acid ($HBF_4$, 40%, Meryer).

### Synthesis and crystal growth

The colorless block crystals of MPZ-$NH_4$-$(BF_4)_3$ were obtained by evaporation of aqueous solutions containing Methylpiperazine (10 mmol), $NH_4BF_4$ (10 mmol) and $HBF_4$ (20 mmol) at 333 K. The collected crystals were dried and weighed to 2.712 g. The purity of the crystals was confirmed by PXRD and the calculated yield was 71.2%. Repeating the above synthesis steps also yielded colorless block crystals of MPZ-$NH_4$-$(BF_4)_3$, the purity of which was checked by PXRD and the yield was calculated to be 70.8%.

### X-ray single crystal diffraction

Single crystal X-ray diffraction data of MPZ-$NH_4$-$(BF_4)_3$ were collected on a Bruker D8 Venture diffractometer with Cu-Kα (λ = 1.54184 Å) radiation, equipped with a temperature controller. Data processing was carried out using APEX-III software. The crystal structures were solved by SHELXT methods with the Olex2 1.5 software package, and all non-hydrogen atoms were refined anisotropically by least-squares technique on weighted $F^2$. Crystallographic data for MPZ-$NH_4$-$(BF_4)_3$ at 303 K and 393 K have been deposited at the Cambridge Crystallographic Data Centre (CCDC) under deposition numbers 2416312 and 2416313, respectively.

### Determination and fixation methods of crystal orientation

The process for determining the *a*-axis direction of the MPZ-$NH_4$-$(BF_4)_3$ single crystal is as follows. First, the MPZ-$NH_4$-$(BF_4)_3$ single crystal was selected and mounted on a suitable holder of the Bruker D8 VENTURE diffractometer as shown in Fig. S3. Then, after performing the unit cell parameter scan (Figs. S4a-b), the Orient Crystal program was selected. The steps shown in Fig. S4c were performed. After entering the commands, the Bruker D8 VENTURE diffractometer completed the orientation adjustment as shown in Fig. S4d. Finally, the MPZ-$NH_4$-$(BF_4)_3$ single crystal was taken down, cut into a suitable shape, and prepared for dielectric testing. The *b*-axis and *c*-axis directions of the MPZ-$NH_4$-$(BF_4)_3$ single crystal were determined in the same way.

As shown in Fig. S6, the MPZ-$NH_4$-$(BF_4)_3$ single crystal was carefully fixed to the IC socket using suitably sized copper wires and silver glue. Finally, the IC socket was connected to a Tonghui TH2828A instrument, and the dielectric constant was measured at frequencies ranging from 500 Hz to 1 MHz, while heating and cooling at a rate of 10 K $min^{-1}$.

### Dielectric measurements

First, the crystals were ground into powder using an agate mortar. Then, an amount of the powder was put into the mold and compressed under the pressure of 60 MPa to form a circular sheet approximately 0.5 mm thick. After that, the sheet was cut into 3 × 4 $mm^2$ square blocks for testing. Next, a simple capacitor was prepared by fixing the small sheet on the IC socket using 7 mm copper wires and silver glue. Finally, the IC socket was connected to a Tonghui TH2828A instrument, and

the dielectric constant was measured at frequencies ranging from 500 Hz to 1 MHz, while heating and cooling at a rate of 10 K $min^{-1}$.

**Differential scanning calorimetry (DSC) measurements**

Differential scanning calorimetry measurements were carried out by using a NETZSCH 214 instrument. The powder sample with a mass of about 10 mg was weighed with an analytical balance and placed in an aluminum crucible. The crucible is covered with the matching crucible lid and put onto the instrument The heating and cooling cycles were measured at a rate of 10 K $min^{-1}$ in a nitrogen atmosphere.

**Thermogravimetric analysis (TGA)**

Thermogravimetric analysis was performed by using a NETZSCH STA449 F5 instrument. The powder sample with a mass of about 10 mg was weighed with an analytical balance and placed in a crucible. The crucible was then covered with the appropriate lid and placed in the instrument. TGA was carried out from 300 to 1200 K at a heating rate of 10 K $min^{-1}$ in an air atmosphere.

**Powder X-ray diffraction (PXRD)**

PXRD measurements were performed at room temperature on a D8 Advance 03030502 instrument. A portion of the powder sample was uniformly dispersed on the sample stage used for testing. The diffraction pattern was obtained in the 2θ range of 5~50° with a step size of 0.02°.

**Hirshfeld surfaces analyses**

Hirshfeld surfaces and the corresponding 2D fingerprint plots were obtained by using a CrystalExplorer program with inputting CIF files, and all results were generated based on standard surface resolution. The strength of molecular interactions is mapped onto the Hirschfeld surface by using the corresponding white-blue-red scheme: where the white regions correspond to distances close to the van der Waals contact, the blue regions indicate longer contacts, and the red regions represent closer contacts.

**The calculation of $\Delta S$ and $N$**

$$\Delta S = \int_{T'}^{T} \frac{Q}{T} dT \approx \frac{\Delta H}{T}$$

$$= \frac{7.65\ J \cdot g^{-1} \times 380.65\ g \cdot mol^{-1}}{382\ K}$$

$$= 7.62\ J \cdot mol^{-1} \cdot K^{-1}$$

$$\Delta S = R \ln N$$

$$N = e^{\left(\frac{\Delta s}{R}\right)}$$

$$= e^{\left(\frac{7.62\ J \cdot mol^{-1} \cdot K^{-1}}{8.314\ J \cdot mol^{-1} \cdot K^{-1}}\right)}$$

$= 2.51$

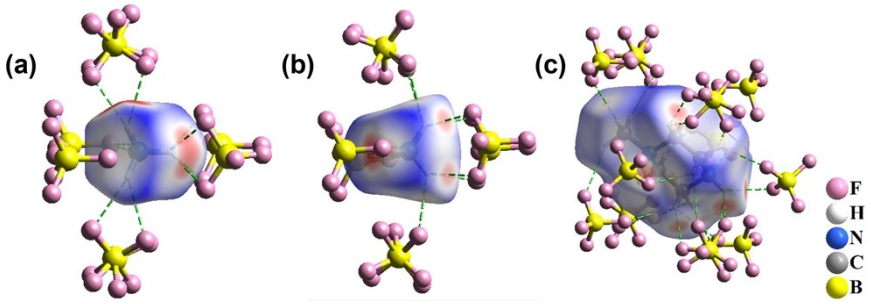


**Fig. S1** Crystal structures of MPZ-$NH_4$-$(BF_4)_3$ in the LTP. (a and b) Hirshfeld surfaces of $NH_4^+$ reflecting the interactions between $NH_4^+$ and $BF_4^-$. (c) The Hirshfeld surface of $MPZ^{2+}$ reflecting the interactions between $MPZ^{2+}$ and $BF_4^-$. Green dashed lines represent N–H···F and C–H···F hydrogen bonds.

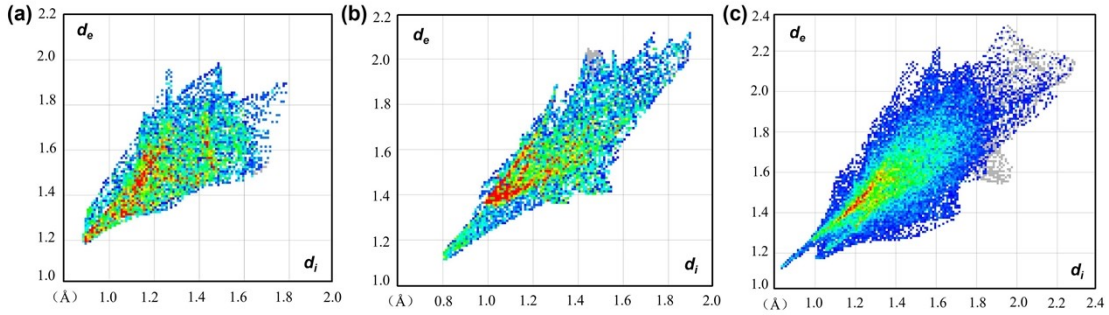


**Fig. S2** (a) 2D fingerprint plot of $NH_4^+$ in the LTP. (b) 2D fingerprint plot of $NH_4^+$ in the LTP. (c) 2D fingerprint plot of $MPZ^{2+}$ in the LTP.

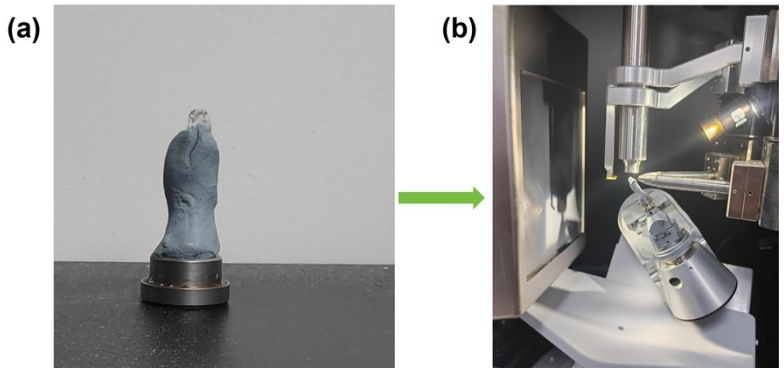


**Fig. S3** The MPZ-$NH_4$-$(BF_4)_3$ single crystal was mounted in a suitable holder (a) and fixed to the Bruker D8 VENTURE diffractometer (b).

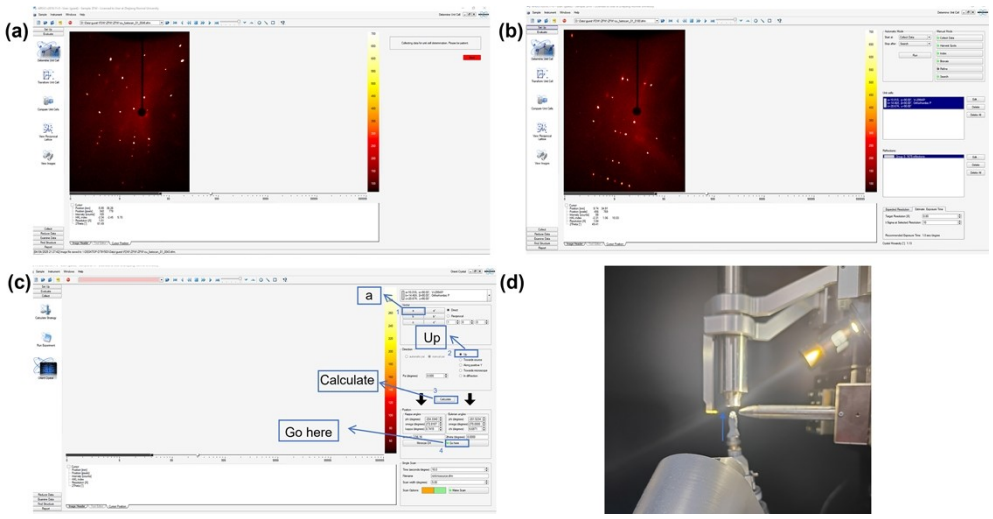


**Fig. S4** The process of using the Orient Crystal program to determine the *a*-axis direction of MPZ-$NH_4$-$(BF_4)_3$.

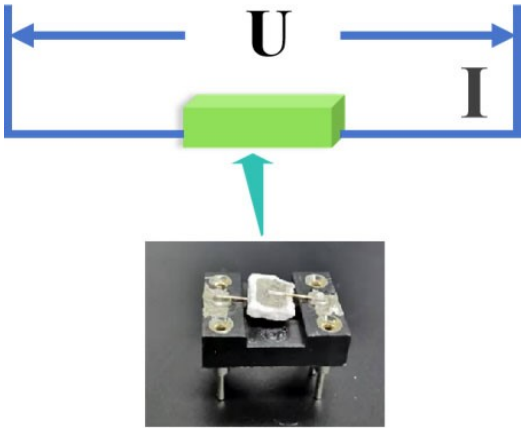


**Fig. S5** Schematic diagram of dielectric measurements for powder samples.

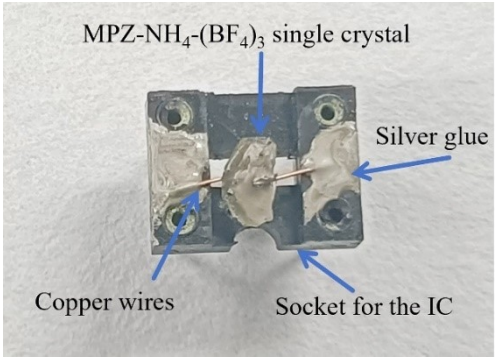


**Fig. S6** The photograph of the MPZ-$NH_4$-$(BF_4)_3$ single crystal mounted on the IC socket.

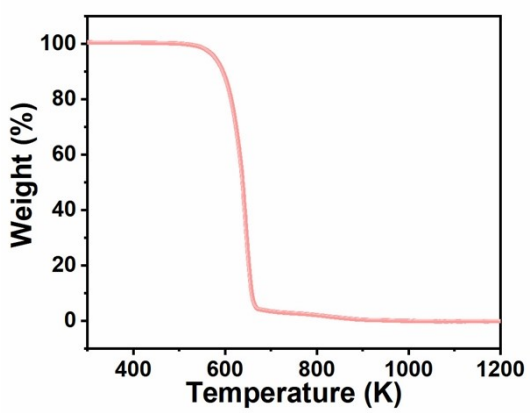


**Fig. S7** TGA of MPZ-$NH_4$-$(BF_4)_3$ from 300 K to 1200 K.

**Table S1** Crystal data and structure refinement data for MPZ-$NH_4$-$(BF_4)_3$

| Compound | MPZ-$NH_4$-$(BF_4)_3$ | MPZ-$NH_4$-$(BF_4)_3$ |
|---|---|---|
| Temperature | 303 K | 393 K |
| CCDC number | 2416312 | 2416313 |
| Formula | $C_5H_{18}B_3F_{12}N_3$ | $C_5H_{18}B_3F_{12}N_3$ |
| Formula weight | 380.65 | 380.65 |
| Crystal system | Orthorhombic | Orthorhombic |
| Space group | *Pnma* | *Cmcm* |
| *a* (Å) | 10.064(2) | 10.449(3) |
| *b* (Å) | 14.486(2) | 10.169(3) |
| *c* (Å) | 20.686(6) | 14.541(6) |
| *α* (°) | 90 | 90 |
| *β* (°) | 90 | 90 |
| *γ* (°) | 90 | 90 |
| *V* (Å$^3$) | 3015.5(12) | 1545.1(9) |
| *Z* | 8 | 4 |
| Density (g cm$^{-3}$) | 1.677 | 1.558 |
| $R_{int}$ | 0.0990 | 0.0741 |
| $R_1$ | 0.1126 | 0.1458 |
| $wR_2$ | 0.2669 | 0.3346 |
| GOF | 1.103 | 1.007 |

**Table S2** Hydrogen bond distances and angles of MPz-$NH_4$-$(BF_4)_3$ at 303 K.

| *D*—H···*A* | *D*—H (Å) | H···*A* (Å) | *D*···*A* (Å) | *D*—H···*A* (°) |
|---|---|---|---|---|
| N1—H1*C*···F4$^{iii}$ | 0.89 | 2.45 | 2.986 (5) | 120 |
| N1—H1*C*···F4$^{iv}$ | 0.89 | 2.45 | 2.986 (5) | 120 |
| N1—H1*C*···F12$^{v}$ | 0.89 | 2.39 | 2.999 (6) | 126 |
| N1—H1*C*···F12$^{vi}$ | 0.89 | 2.39 | 2.999 (6) | 126 |
| N1—H1*D*···F13 | 0.89 | 2.63 | 3.216 (8) | 125 |
| N1—H1*D*···F15 | 0.89 | 2.20 | 3.014 (10) | 152 |
| N1—H1*D*···F2 | 0.89 | 2.25 | 2.970 (7) | 137 |

| | | | | |
|---|---|---|---|---|
| N1—H1*D*···F17 | 0.89 | 2.63 | 3.155 (10) | 118 |
| N1—H1*E*···F13$^{i}$ | 0.89 | 2.63 | 3.216 (8) | 125 |
| N1—H1*E*···F15$^{i}$ | 0.89 | 2.20 | 3.014 (10) | 152 |
| N1—H1*E*···F2$^{i}$ | 0.89 | 2.25 | 2.970 (7) | 137 |
| N1—H1*E*···F17$^{i}$ | 0.89 | 2.63 | 3.155 (10) | 118 |
| N1—H1*F*···F6 | 0.89 | 2.20 | 3.018 (7) | 154 |
| N4—H4*C*···F18 | 0.89 | 2.11 | 2.914 (8) | 150 |
| N4—H4*C*···F11 | 0.89 | 2.52 | 3.351 (10) | 156 |
| N4—H4*D*···F8$^{vii}$ | 0.89 | 2.43 | 3.022 (6) | 124 |
| N4—4*D*···F16$^{viii}$ | 0.89 | 2.41 | 3.002 (6) | 124 |
| N4—H4*D*···F3 | 0.89 | 2.56 | 3.017 (11) | 112 |
| N4—H4*D*···F9 | 0.89 | 2.45 | 3.110 (12) | 131 |
| N4—H4*D*···F19 | 0.89 | 2.52 | 3.182 (11) | 132 |
| N4—H4*E*···F8$^{ix}$ | 0.89 | 2.43 | 3.022 (6) | 124 |
| N4—H4*E*···F16$^{x}$ | 0.89 | 2.41 | 3.002 (6) | 124 |
| N4—H4*E*···F3$^{ii}$ | 0.89 | 2.56 | 3.017 (11) | 112 |
| N4—H4*E*···F9$^{ii}$ | 0.89 | 2.45 | 3.110 (12) | 131 |
| N4—H4*E*···F19$^{ii}$ | 0.89 | 2.52 | 3.182 (11) | 132 |
| N4—H4*F*···F5 | 0.89 | 2.02 | 2.792 (8) | 145 |
| N2—H2···F8$^{vii}$ | 0.98 | 2.60 | 3.323 (6) | 131 |
| N2—H2···F16$^{viii}$ | 0.98 | 2.27 | 3.131 (6) | 146 |
| N3—H3*A*···F1 | 0.89 | 2.33 | 3.044 (5) | 137 |
| N3—H3*A*···F13 | 0.89 | 2.25 | 2.945 (8) | 134 |
| N3—H3*A*···F15 | 0.89 | 2.38 | 3.039 (12) | 131 |
| N3—H3*B*···F20$^{vii}$ | 0.89 | 2.06 | 2.875 (6) | 152 |
| C1—H1*B*···F12$^{vii}$ | 0.97 | 2.36 | 3.309 (8) | 165 |
| C4—H4*A*···F7$^{viii}$ | 0.97 | 2.49 | 3.244 (10) | 135 |
| C4—H4*A*···F19$^{viii}$ | 0.97 | 2.36 | 3.190 (11) | 144 |
| C4—H4*B*···F4$^{viii}$ | 0.97 | 2.42 | 3.300 (7) | 150 |
| C5—H5*A*···F4 | 0.97 | 2.62 | 3.315 (7) | 129 |
| C5—H5*A*···F17$^{viii}$ | 0.97 | 2.55 | 3.250 (12) | 129 |
| C5—H5*B*···F16$^{viii}$ | 0.97 | 2.47 | 3.258 (8) | 138 |
| C5—H5*B*···F19 | 0.97 | 2.61 | 3.429 (12) | 142 |
| C3—H3*C*···F9$^{vii}$ | 0.97 | 2.56 | 3.240 (13) | 127 |
| C3—H3*D*···F8$^{vii}$ | 0.97 | 2.53 | 3.264 (9) | 133 |
| C3—H3*D*···F15 | 0.97 | 2.55 | 3.032 (12) | 111 |
| C3—H3*D*···F9 | 0.97 | 2.36 | 3.251 (14) | 152 |
| C2—H2*A*···F2$^{xi}$ | 0.96 | 2.49 | 3.438 (11) | 172 |
| C2—H2*A*···F17$^{xi}$ | 0.96 | 2.55 | 3.399 (12) | 148 |
| C2—H2*B*···F18$^{xi}$ | 0.96 | 2.56 | 3.430 (9) | 150 |
| C2—H2*C*···F10$^{vii}$ | 0.96 | 2.60 | 3.379 (8) | 139 |

Symmetry codes: (i) *x*, −*y*+1/2, *z*; (ii) *x*, −*y*+3/2, *z*; (iii) *x*+1/2, *y*, −*z*+1/2; (iv) *x*+1/2, −*y*+1/2, −*z*+1/2; (v) −*x*+2, −*y*+1, −*z*+1; (vi) −*x*+2, *y*−1/2, −*z*+1; (vii) −*x*+1, −*y*+1, −*z*+1; (viii) *x*−1/2, *y*, −*z*+1/2; (ix) −*x*+1, *y*+1/2, −*z*+1; (x) *x*−1/2, −*y*+3/2, −*z*+1/2; (xi) *x*−1, *y*, *z*.

**Table S3** Partial bond lengths and bond angles of MPZ-$NH_4$-$(BF_4)_3$ at 303 K.

| Bond lengths / Å and bond angles / ° | | | |
|---|---|---|---|
| F1—B3 | 1.384 (10) | F5—B4 | 1.297 (10) |
| F4—B3 | 1.382 (5) | F11—B2 | 1.351 (11) |
| F6—B3 | 1.375 (10) | B5—F3 | 1.358 (12) |
| F8—B1 | 1.372 (6) | B5—F13 | 1.368 (10) |
| F10—B1 | 1.361 (9) | B5—F7 | 1.411 (10) |
| F12—B4 | 1.370 (6) | B5—F15 | 1.393 (11) |
| F14—B1 | 1.363 (10) | B5—F2 | 1.375 (10) |
| F16—B2 | 1.354 (6) | B5—F17 | 1.306 (11) |
| F18—B2 | 1.348 (10) | B5—F9 | 1.369 (13) |
| F20—B4 | 1.373 (10) | B5—F19 | 1.372 (11) |
| F10—B1—F8 | 109.9 (5) | F12—B4—F20 | 107.9 (5) |
| F10—B1—F14 | 108.6 (7) | F5—B4—$F12^{ii}$ | 109.9 (5) |
| F14—B1—F8 | 110.0 (5) | F5—B4—F12 | 109.9 (5) |
| F14—B1—$F8^{i}$ | 110.0 (5) | F5—B4—F20 | 113.1 (8) |
| $F12^{ii}$—B4—F12 | 107.9 (6) | F3—B5—F13 | 147.0 (9) |
| $F12^{ii}$—B4—F20 | 107.9 (5) | F3—B5—F2 | 86.3 (8) |
| F11—B2—$F16^{ii}$ | 109.9 (6) | F3—B5—F19 | 100.9 (8) |
| F8—B1—$F8^{i}$ | 108.5 (6) | F13—B5—F2 | 112.0 (7) |
| F10—B1—$F8^{i}$ | 109.9 (5) | F13—B5—F19 | 68.5 (6) |
| F9—B5—F7 | 105.8 (8) | F15—B5—F7 | 164.0 (9) |
| F9—B5—F15 | 79.3 (8) | F4—B3—F1 | 108.9 (5) |
| F19—B5—F2 | 165.1 (9) | $F4^{i}$—B3—F1 | 108.9 (5) |
| F16—B2—$F16^{ii}$ | 110.8 (7) | $F4^{i}$—B3—F4 | 108.0 (6) |
| F18—B2—F16 | 110.4 (6) | F6—B3—F1 | 110.3 (6) |
| F18—B2—$F16^{ii}$ | 110.4 (6) | F6—B3—F4 | 110.3 (5) |
| F18—B2—F11 | 105.3 (8) | F6—B3—$F4^{i}$ | 110.3 (5) |
| F11—B2—F16 | 109.9 (6) | | |

Symmetry codes: (i) $x$, $-y+1/2$, $z$; (ii) $x$, $-y+3/2$, $z$.

**Table S4** Partial bond lengths and bond angles of MPZ-$NH_4$-$(BF_4)_3$ at 393 K

| Bond lengths / Å and bond angles / ° | | | |
|---|---|---|---|
| F1—B1 | 1.324 (8) | $F1^{vi}$—B1—F1 | 110.6 (11) |
| F4—B1 | 1.293 (16) | $F1^{vi}$—B1—F5 | 108.5 (11) |
| B1—F5 | 1.391 (19) | F1—B1—F5 | 108.5 (11) |
| B2—$F3^{i}$ | 1.314 (10) | F4—B1—F1 | 113.6 (11) |
| B2—$F3^{ii}$ | 1.314 (10) | F4—B1—$F1^{vi}$ | 113.6 (11) |
| B2—F3 | 1.314 (10) | F4—B1—F5 | 101.4 (12) |
| B2—$F3^{iii}$ | 1.314 (10) | $F3^{i}$—B2—F3 | 163.3(15) |
| B2—$F2^{i}$ | 1.340 (11) | $F3^{i}$—B2—$F3^{ii}$ | 113.7 (12) |
| B2—F2 | 1.340 (11) | $F3^{iii}$—B2—F3 | 113.7 (12) |
| B2—$F2^{ii}$ | 1.340 (11) | $F3^{iii}$—B2—$F3^{ii}$ | 166.3(15) |

| | | | |
|---|---|---|---|
| B2—F2$^{iii}$ | 1.340 (11) | F3$^{i}$—B2—F3$^{iii}$ | 66.3 (12) |
| F3—B2—F3ii | 66.3 (12) | F3ii—B2—F2iii | 109.7 (7) |
| F3$^{i}$—B2—F2$^{iii}$ | 107.1 (7) | F3—B2—F2$^{ii}$ | 107.1 (7) |
| F3$^{iii}$—B2—F2$^{ii}$ | 109.7 (7) | F3$^{i}$—B2—F2$^{i}$ | 70.3 (7) |
| F3$^{ii}$—B2—F2$^{i}$ | 72.9 (7) | F3—B2—F2$^{i}$ | 109.7 (7) |
| F3$^{iii}$—B2—F2$^{iii}$ | 70.3 (7) | F3$^{iii}$—B2—F2$^{i}$ | 107.1 (7) |
| F3$^{ii}$—B2—F2$^{ii}$ | 70.3 (7) | F2$^{iii}$—B2—F2 | 109.6 (12) |
| F3—B2—F2$^{iii}$ | 72.9 (7) | F2$^{i}$—B2—F2 | 168.3(15) |
| F3$^{i}$—B2—F2$^{ii}$ | 72.9 (7) | | |

Symmetry codes: (i) −*x*+1, −*y*+2, −*z*+1; (ii) −*x*+1, *y*, *z*; (iii) *x*, −*y*+2, −*z*+1; (iv) −*x*+1, −*y*+1, −*z*+1; (v) *x*, −*y*+1, −*z*+1; (vi) *x*, *y*, −*z*+3/2

**Table S5** The distance between the N and B atoms in the $(NH_4)(BF_4)_6$ octahedra at 303 K.

| Atom | Atom | Distance/ Å | Atom | Atom | Distance/ Å |
|---|---|---|---|---|---|
| N1 | B5 | 3.6407 (74) | N1 | B5 | 3.6407 (74) |
| N1 | B1 | 3.6285 (94) | N1 | B3 | 3.5753 (99) |
| N1 | B4 | 3.5793 (94) | N1 | B3 | 3.6168 (98) |
| N4 | B5 | 3.7417 (73) | N4 | B5 | 3.7417 (73) |
| N4 | B2 | 3.7530 (109) | N4 | B1 | 3.5893 (94) |
| N4 | B2 | 3.5284 (106) | N4 | B4 | 3.9931 (94) |

**Table S6** The distance between the N and B atoms in the $(NH_4)(BF_4)_6$ octahedra at 393 K.

| Atom | Atom | Distance/ Å | Atom | Atom | Distance/ Å |
|---|---|---|---|---|---|
| N1 | B1 | 3.7625 (179) | N1 | B1 | 3.7625 (179) |
| N1 | B2 | 3.6918 (20) | N1 | B2 | 3.6918 (20) |
| N1 | B1 | 3.5834 (180) | N1 | B1 | 3.5834 (180) |